

# Uncertainties in nuclear transition matrix elements for $\beta^+\beta^+$ and $\varepsilon\beta^+$ modes of neutrinoless positron double- $\beta$ decay within PHFB model

P. K. Rath<sup>1</sup>, R. Chandra<sup>2</sup>, K. Chaturvedi<sup>3</sup>, P. Lohani<sup>1</sup>, P. K. Raina<sup>4</sup> and J. G. Hirsch<sup>5</sup>

<sup>1</sup>Department of Physics, University of Lucknow, Lucknow-226007, India

<sup>2</sup>Department of Applied Physics, Babasaheb Bhimrao Ambedkar University, Lucknow-226025, India

<sup>3</sup>Department of Physics, Bundelkhand University, Jhansi-284128, India

<sup>4</sup>Department of Physics, Indian Institute of Technology, Ropar, Rupnagar - 140001, Punjab, India

<sup>5</sup>Instituto de Ciencias Nucleares, Universidad Nacional Autónoma de México, 04510 México, D.F., México

(Dated: December 21, 2012)

Uncertainties in the nuclear transition matrix elements  $M^{(0\nu)}$  and  $M^{(0N)}$  of the double-positron emission  $(\beta^+\beta^+)_{0\nu}$  and electron-positron conversion  $(\varepsilon\beta^+)_{0\nu}$  modes due to the exchange of light and heavy Majorana neutrinos, respectively, are calculated for  $^{96}\text{Ru}$ ,  $^{102}\text{Pd}$ ,  $^{106}\text{Cd}$ ,  $^{124}\text{Xe}$ ,  $^{130}\text{Ba}$  and  $^{156}\text{Dy}$  isotopes by employing the PHFB model with four different parameterization of the pairing plus multipolar two-body interactions and three different parameterizations of the Jastrow short range correlations. In all cases but for  $^{130}\text{Ba}$ , the uncertainties are smaller than 14% for light Majorana neutrino exchange and 35% for the exchange of a heavy Majorana neutrino.

PACS numbers: 21.60.Jz, 23.20.-g, 23.40.Hc

## I. INTRODUCTION

The Majorana nature of the neutrinos could be immediately established by confirming the possible occurrence of any one out of four experimentally distinguishable modes of lepton number violating neutrinoless double beta  $(\beta\beta)_{0\nu}$  decay, namely the double-electron emission  $(\beta^-\beta^-)_{0\nu}$ , double-positron emission  $(\beta^+\beta^+)_{0\nu}$ , electron-positron conversion  $(\varepsilon\beta^+)_{0\nu}$  and double-electron capture  $(\varepsilon\varepsilon)_{0\nu}$ . The latter three modes are energetically competing and we shall refer to them as  $(e^+\beta\beta)_{0\nu}$  decay. The kinetic energy release in the  $(\varepsilon\varepsilon)_{0\nu}$  mode is the largest. However, the conservation of energy-momentum requires the emission of an additional particle in the  $(\varepsilon\varepsilon)_{0\nu}$  mode. The absorption of atomic electrons from the  $K$ -shell is forbidden for the  $0^+ \rightarrow 0^+$  transition due to the emission of one real photon. Consequently, various processes such as internal pair production, internal conversion, emission of two photons,  $L$ -capture etc. [1] have to be considered. The decay rates of the above mentioned processes have to be calculated at least by the third order perturbation theory and are suppressed by a factor of the order of  $10^{-4}$  in comparison to the  $(\varepsilon\beta^+)_{0\nu}$  mode. Hence, the experimental as well as theoretical studies of  $(e^+\beta\beta)_{0\nu}$  decay had been mostly restricted to  $(\beta^+\beta^+)_{0\nu}$  and  $(\varepsilon\beta^+)_{0\nu}$  modes only.

The idea behind the resonant enhancement of  $(\varepsilon\varepsilon)_{0\nu}$  mode [2–5], has been recently reanalyzed [6, 7] and it has been shown that there will be resonant enhancement of the  $(\varepsilon\varepsilon)_{0\nu}$  mode upto a factor of  $10^6$  provided the nuclear levels in the parent and daughter nuclei are almost degenerate i.e.  $Q - (E_{2P} - E_{2S}) \sim 1 \text{ keV}$ , where the energy difference is for atomic levels. Subsequently, detailed theoretical studies on the resonant enhancement of  $(\varepsilon\varepsilon)_{0\nu}$  mode have also been performed [8, 9]. In the mean time, experimental studies on resonance enhancement of  $(\varepsilon\varepsilon)_{0\nu}$  mode in  $^{74}\text{Ge}$  [10, 11],  $^{96}\text{Ru}$  [12],  $^{106}\text{Cd}$  [13, 14],  $^{112}\text{Sn}$  [15–19],  $^{136}\text{Ce}$  [20] and  $^{180}\text{W}$  [21] isotopes have al-

ready been carried out and the study of this  $(\varepsilon\varepsilon)_{0\nu}$  mode is emerging as an interesting possibility for the investigation of  $(\beta\beta)_{0\nu}$  decay.

In addition to establishing the Dirac or Majorana nature of neutrinos, the observation of  $(\beta\beta)_{0\nu}$  decay can also ascertain the role of various mechanisms in different gauge theoretical models [22]. The study of  $(\beta\beta)_{0\nu}$  decay can clarify a number of issues, such as the origin of the neutrino mass, their absolute scale as well as hierarchy, and possible CP violation in the leptonic sector. The  $(\beta\beta)_{0\nu}$  and  $(e^+\beta\beta)_{0\nu}$  decay modes can provide us with similar but complementary information. The observation of  $(e^+\beta\beta)_{0\nu}$  decay modes would be helpful in determining the presence of mass mechanism or right handed currents [23]. The varied scope and far reaching nature of the experimental and theoretical studies on the  $(\beta\beta)_{0\nu}$  decay have been recently reviewed by Avignone *et al.* [24], Vergados *et al.* [25] and Faessler *et al.* [26]

The nuclear  $\beta\beta$  decay proceeds through strongly suppressed channels which are very sensitive to details of the wave functions of the parent, intermediate and daughter nuclei. Hence, the calculations of non-collective nuclear  $\beta\beta$  decay related observables are quite challenging. In any nuclear model, there are three basic ingredients, namely the model space, the single particle energies (SPEs) and the effective two body interactions. Usually, these are chosen on the basis of practical considerations. While all models are able to reproduce most of the observed  $(\beta\beta)_{2\nu}$  decay half lives by adjusting free parameters in the model, different predictions are obtained for other observables, like the  $(\beta\beta)_{0\nu}$  decay half lives, due to the inherent freedom in choosing the basic ingredients of the model.

A variety of nuclear models is currently employed in this endeavor. Large scale shell model calculations are quite successful [27–29], but highly limited in the description of medium and heavy mass nuclei. The most popular and successful model is the Quasiparticle Random Phase

Approximation (QRPA) and its extensions [30, 31]. The inclusion of nuclear deformation has also been carried out in the deformed QRPA [32, 33], the Projected Hartree-Fock-Bogoliubov (PHFB) [34–36], the pseudo-SU(3) [37], the Interacting Boson Model (IBM) [38], and the Energy Density Functional (EDF) [39] approaches. In the study of both  $(\beta\beta)_{2\nu}$  and  $(\beta\beta)_{0\nu}$  decay modes, the renormalized value of axial vector coupling constant  $g_A$  is a major source of uncertainty. In the  $(\beta\beta)_{0\nu}$  decay, the role of pseudoscalar and weak magnetism terms [40, 41] is crucial, and the finite size of nucleons (FNS) and short range correlations (SRC) play a decisive role vis-a-vis the radial evolution of nuclear transition matrix elements (NTMEs) [28, 35, 36, 42].

Usually, three different approaches have been adopted for estimating the uncertainties in NTMEs for  $(\beta^-\beta^-)_{0\nu}$  decay. The spread between all the available calculated NTMEs has been used as the measure of the theoretical uncertainty [43]. The same spread between NTMEs can also be translated into average and standard deviation, which can be interpreted as theoretical uncertainty [44, 45]. According to Bilenky and Grifols [46], the observation of  $(\beta\beta)_{0\nu}$  decay of different nuclei will provide a method, in which the ratios of the NTMEs-squared can be compared with the ratios of observed half-lives  $T_{1/2}^{0\nu}$  and the results of calculations of NTMEs can be checked in a model independent way.

The theoretical uncertainties were estimated by Rodin *et al.* [47] by considering two models, QRPA and RQRPA, with three sets of basis states and three realistic two-body effective interactions based on the charge dependent Bonn, Argonne and Nijmen potentials. It was found that the variances were substantially smaller than the average values and the results of QRPA, albeit slightly larger, are quite close to the RQRPA values. The critical analysis of the advantages and deficiencies in the approach of Rodin *et al.* [47] by Suhonen [48] and Rodin *et al.* [49] is quite instructive. Further studies on the uncertainties in NTMEs due to SRC using the unitary correlation operator method (UCOM) [50] and by self-consistent coupled cluster method (CCM) [51] have also been carried out.

Recently, the uncertainties in the  $(\beta^-\beta^-)_{0\nu}$  NTMEs due to the exchange of light [35] and heavy [36] Majorana neutrinos have been calculated in the PHFB model by

employing four different parameterizations of the pairing plus multipolar effective two body interaction and three different parameterizations of Jastrow type of SRC. In the present work, we employ the same formalism for estimating uncertainties in NTMEs for  $(\varepsilon\beta^+)_{0\nu}$  and  $(\varepsilon\varepsilon)_{0\nu}$  modes of  $^{96}\text{Ru}$ ,  $^{102}\text{Pd}$ ,  $^{106}\text{Cd}$ ,  $^{124}\text{Xe}$ ,  $^{130}\text{Ba}$  and  $^{156}\text{Dy}$  isotopes for the  $0^+ \rightarrow 0^+$  transition. The article is organized as follows. A brief discussion of the theoretical formalism is presented in Sec. II. In Sec. III, we analyze the role of the different parameterizations of the two body interaction, the finite size of nucleons and higher order currents (HOC). The influence of the SRC in the radial evolution of the NTMEs is also presented. In the same Sec. III, we estimate the uncertainties, which are subsequently employed for extracting bounds on the effective mass of light neutrinos  $\langle m_\nu \rangle$  and heavy neutrinos  $\langle M_N \rangle$ . In Sec. IV, the conclusions are presented.

## II. THEORETICAL FORMALISM

In the Majorana neutrino mass mechanism, the half-lives  $T_{1/2}^{0\nu}$  for the  $0^+ \rightarrow 0^+$  transition of  $(\beta^+\beta^+)_{0\nu}$  and  $(\varepsilon\beta^+)_{0\nu}$  modes are given by [1, 40, 41]

$$\left[ T_{1/2}^{0\nu}(\beta) \right]^{-1} = G_{01}(\beta) \left| \frac{\langle m_\nu \rangle}{m_e} M^{(0\nu)} + \frac{m_p}{\langle M_N \rangle} M^{(0N)} \right|^2. \quad (1)$$

Here,  $\beta$  denotes the  $(\beta^+\beta^+)_{0\nu} / (\varepsilon\beta^+)_{0\nu}$  modes,

$$\langle m_\nu \rangle = \sum_i' U_{ei}^2 m_i, \quad m_i < 10 \text{ eV}, \quad (2)$$

$$\langle M_N \rangle^{-1} = \sum_i'' U_{ei}^2 m_i^{-1}, \quad m_i > 1 \text{ GeV}. \quad (3)$$

and

$$M^{(K)} = -\frac{M_F^{(K)}}{g_A^2} + M_{GT}^{(K)} + M_T^{(K)} \quad (4)$$

where  $K = 0\nu (0N)$  denotes the exchange of light (heavy) Majorana neutrino mechanism.

In the PHFB model, the NTMEs  $M^{(K)}$  for the  $(\beta^+\beta^+)_{0\nu}$  and  $(\varepsilon\beta^+)_{0\nu}$  modes are calculated by employing the closure approximation [34]

$$\begin{aligned} M^{(K)} &= \langle \Psi_{00}^{J_f=0} || O^{(K)} || \Psi_{00}^{J_i=0} \rangle \\ &= [n_{Z,N}^{J_i=0} n_{Z-2,N+2}^{J_f=0}]^{-1/2} \int_0^\pi n_{(Z,N),(Z-2,N+2)}(\theta) \sum_{\alpha\beta\gamma\delta} \left( \alpha\beta \left| O^{(K)} \right| \gamma\delta \right) \\ &\quad \times \sum_{\varepsilon\eta} \frac{(f_{Z-2,N+2}^{(\nu)*})_{\varepsilon\beta}}{\left[ 1 + F_{Z,N}^{(\nu)}(\theta) f_{Z-2,N+2}^{(\nu)*} \right]_{\varepsilon\alpha}} \frac{(F_{Z,N}^{(\pi)*})_{\eta\delta}}{\left[ 1 + F_{Z,N}^{(\pi)}(\theta) f_{Z-2,N+2}^{(\pi)*} \right]_{\eta\gamma}} \sin\theta d\theta \end{aligned} \quad (5)$$

where

$$O^{(K)} = \left[ -\frac{H_F^{(K)}(r_{nm})}{g_A^2} + \sigma_n \cdot \sigma_m H_{GT}^{(K)}(r_{nm}) + S_{12} H_T^{(K)}(r_{nm}) \right] \tau_n^+ \tau_m^+ \quad (6)$$

with

$$S_{nm} = 3 (\sigma_n \cdot \hat{\mathbf{r}}_{nm}) (\sigma_m \cdot \hat{\mathbf{r}}_{nm}) - \sigma_n \cdot \sigma_m \quad (7)$$

and the expressions for  $n^J$ ,  $n_{(Z,N),(Z-2,N+2)}(\theta)$ ,  $f_{Z,N}$  and  $F_{Z,N}(\theta)$  are given in Ref. [34]. The three components of the nuclear transition matrix element  $M^{(K)}$  are denoted by  $F$ ,  $GT$  and  $T$  corresponding to Fermi, Gamow-Teller and tensor terms.

The neutrino potentials due to the exchange of light and heavy neutrinos between nucleons having finite size are given by

$$H_\alpha^{(0\nu)}(r_{nm}) = \frac{2R}{\pi} \int \frac{f_\alpha(qr_{nm})}{(q+A)} h_\alpha(q) q dq \quad (8)$$

$$H_\alpha^{(0N)}(r_{nm}) = \frac{2R}{(m_p m_e) \pi} \int f_\alpha(qr_{nm}) h_\alpha(q) q^2 dq \quad (9)$$

where  $f_\alpha(qr_{nm}) = j_0(qr_{nm})$  for  $\alpha = F, GT$  and  $f_\alpha(qr_{nm}) = j_2(qr_{nm})$  for  $\alpha = T$ . The above expressions for the NTMEs  $M^{(K)}$  were obtained by including pseudoscalar and weak magnetism terms in the nucleonic current and employing the Goldberger-Treiman PCAC relation for the induced pseudoscalar term [40].

Usually, the influence of the finite size of nucleons (FNS) is taken into account through dipole form factors. The functions  $h_F(q)$ ,  $h_{GT}(q)$  and  $h_T(q)$  are written as

$$h_F(q) = g_V^2(q^2) \quad (10)$$

$$h_{GT}(q) = \frac{g_A^2(q^2)}{g_A^2} \left[ 1 - \frac{2}{3} \frac{g_P(q^2)q^2}{g_A(q^2)2m_p} + \frac{1}{3} \frac{g_P^2(q^2)q^4}{g_A^2(q^2)4m_p^2} \right] + \frac{2}{3} \frac{g_M^2(q^2)q^2}{g_A^2 4m_p^2} \\ \approx \left( \frac{\Lambda_A^2}{q^2 + \Lambda_A^2} \right)^4 \left[ 1 - \frac{2}{3} \frac{q^2}{(q^2 + m_\pi^2)} + \frac{1}{3} \frac{q^4}{(q^2 + m_\pi^2)^2} \right] + \left( \frac{g_V}{g_A} \right)^2 \frac{\kappa^2 q^2}{6m_p^2} \left( \frac{\Lambda_V^2}{q^2 + \Lambda_V^2} \right)^4 \quad (11)$$

$$h_T(q) = \frac{g_A^2(q^2)}{g_A^2} \left[ \frac{2}{3} \frac{g_P(q^2)q^2}{g_A(q^2)2m_p} - \frac{1}{3} \frac{g_P^2(q^2)q^4}{g_A^2(q^2)4m_p^2} \right] + \frac{1}{3} \frac{g_M^2(q^2)q^2}{g_A^2 4m_p^2} \\ \approx \left( \frac{\Lambda_A^2}{q^2 + \Lambda_A^2} \right)^4 \left[ \frac{2}{3} \frac{q^2}{(q^2 + m_\pi^2)} - \frac{1}{3} \frac{q^4}{(q^2 + m_\pi^2)^2} \right] + \left( \frac{g_V}{g_A} \right)^2 \frac{\kappa^2 q^2}{12m_p^2} \left( \frac{\Lambda_V^2}{q^2 + \Lambda_V^2} \right)^4 \quad (12)$$

where

$$g_V(q^2) = g_V \left( \frac{\Lambda_V^2}{q^2 + \Lambda_V^2} \right)^2 \\ g_A(q^2) = g_A \left( \frac{\Lambda_A^2}{q^2 + \Lambda_A^2} \right)^2 \\ g_M(q^2) = \kappa g_V(q^2) \\ g_P(q^2) = \frac{2m_p g_A(q^2)}{(q^2 + m_\pi^2)} \left( \frac{\Lambda_A^2 - m_\pi^2}{\Lambda_A^2} \right) \quad (13)$$

with  $g_V = 1.0$ ,  $g_A = 1.254$ ,  $\kappa = \mu_p - \mu_n = 3.70$ ,  $\Lambda_V = 0.850$  GeV and  $\Lambda_A = 1.086$  GeV.

Consideration of Eq. (6)–Eq. (12) and Eq. (5) implies that the Fermi matrix element  $M_F^{(K)}$  has one term

$-g_A^2 M_{F-VV}^{(K)}$ , the Gamow-Teller matrix element  $M_{GT}^{(K)}$  has four terms, namely  $M_{GT-AA}^{(K)}$ ,  $M_{GT-AP}^{(K)}$ ,  $M_{GT-PP}^{(K)}$ ,  $M_{GT-MM}^{(K)}$  and there are three terms  $M_{T-AP}^{(K)}$ ,  $M_{T-PP}^{(K)}$ ,  $M_{T-MM}^{(K)}$  associated with the tensor matrix element  $M_T^{(K)}$ .

In the literature, the short range correlations (SRC) have been included through the exchange of  $\omega$ -meson [37], effective transition operator [52], unitary correlation operator method (UCOM) [42, 50], self-consistent CCM [51] and phenomenological Jastrow type of correlations with Miller-Spenser parameterization [53]. Further, Šimković *et al.* [51] have shown that in the self-consistent CCM, it is possible to parametrize the effects of Argonne V18 and CD-Bonn nucleon-nucleon ( $NN$ ) potentials by the

Jastrow correlations with Miller-Spenser type of parameterization given by

$$f(r) = 1 - ce^{-ar^2}(1 - br^2). \quad (14)$$

In the present work, the above form is adopted with  $a = 1.1 \text{ fm}^{-2}$ ,  $1.59 \text{ fm}^{-2}$ ,  $1.52 \text{ fm}^{-2}$ ,  $b = 0.68 \text{ fm}^{-2}$ ,  $1.45 \text{ fm}^{-2}$ ,  $1.88 \text{ fm}^{-2}$  and  $c = 1.0, 0.92, 0.46$  for Miller-Spencer parameterization, Argonne V18 and CD-Bonn  $NN$  Potentials, which are denoted as SRC1, SRC2 and SRC3, respectively.

The NTMEs  $M^{(K)}$  of the  $(\beta^+\beta^+)_{0\nu}/(\varepsilon\beta^+)_{0\nu}$  decay mode in the PHFB model have been already discussed in Ref. [34]. The same formalism is employed here. The axially symmetric HFB intrinsic state  $|\Phi_0\rangle$  with  $K = 0$  specified completely by the amplitudes  $(u_{im}, v_{im})$  and expansion coefficients  $C_{ij,m}$ , is obtained by minimizing the expectation value of the effective Hamiltonian given by [54]

$$H = H_{sp} + V(P) + V(QQ) + V(HH), \quad (15)$$

in a basis constructed by using a set of deformed states. Here,  $H_{sp}$  denotes the single particle Hamiltonian and  $V(P)$ ,  $V(QQ)$  and  $V(HH)$  are the pairing, quadrupole-quadrupole and hexadecapole-hexadecapole parts of the effective two-body interaction, respectively.

The details about the parameters of the pairing force  $G_{pp}$  and  $G_{nn}$  as well as three strength parameters of quadrupolar interaction, namely the proton-proton  $\chi_{2pp}$ , the neutron-neutron  $\chi_{2nn}$  and the proton-neutron  $\chi_{2pn}$  have been given in Refs. [34, 55, 56]. Specifically,  $\chi_{2pp} = \chi_{2nn} = 0.0105 \text{ MeV}b^{-4}$ , where  $b$  is the oscillator parameter and the strength parameter  $\chi_{2pn}$  was varied to fit the experimental excitation energy of the  $2^+$  state,  $E_{2+}$ . Presently, we employ in addition an alternative isoscalar parameterization by taking  $\chi_{2pp} = \chi_{2nn} = \chi_{2pn}/2$  and the three parameters are varied together to fit  $E_{2+}$ . These two parameterizations of the quadrupolar interaction are referred as  $PQQ1$  and  $PQQ2$ . The details about the  $HH$  part of the effective interaction  $V(HH)$  have also been given in Ref. [54]. The calculations including the hexadecapolar term  $HH$  are denoted as  $PQQHH$ . With the consideration of the hexadecapolar interaction, we end up with four different parameterizations, namely  $PQQ1$ ,  $PQQHH1$ ,  $PQQ2$  and  $PQQHH2$  of the effective two-body interaction. By employing the four different parameterization of the two body effective interaction and three different parameterizations of SRC, sets of twelve NTMEs  $M^{(0\nu)}$  and  $M^{(0N)}$  for the  $(\beta^+\beta^+)_{0\nu}$  and  $(\varepsilon\beta^+)_{0\nu}$  modes are obtained using Eq. (5) and subsequently, the mean and standard deviations are calculated for estimating uncertainties associated in the results of the present work.

### III. RESULTS AND DISCUSSIONS

In the present work, we use the same model space, single particle energies (SPE's) and parameters of the ef-

fective two-body interaction as our earlier calculations on the  $(e^+\beta\beta)_{2\nu}$  decay of  $^{96}\text{Ru}$ ,  $^{102}\text{Pd}$ ,  $^{106,108}\text{Cd}$  [55],  $^{124,126}\text{Xe}$ ,  $^{130,132}\text{Ba}$  [56] and  $^{156}\text{Dy}$  [57] isotopes for the  $0^+ \rightarrow 0^+$  transition. The calculated yrast spectra, reduced  $B(E2:0^+ \rightarrow 2^+)$  transition probabilities, static quadrupole moments  $Q(2^+)$  and gyromagnetic factors  $g(2^+)$  [55–57] are in an overall agreement with the experimental data due to  $PQQ1$  parameterization. The maximum change in all the calculated spectroscopic properties is about 10% except for the  $B(E2:0^+ \rightarrow 2^+)$  and  $g(2^+)$  of  $^{130}\text{Ba}$ , which change by 19.5% and 16.6%, respectively, employing the other three parameterizations.

#### A. Effects due to finite size of nucleons and short range correlations

The theoretically calculated sets of twelve NTMEs  $M^{(0\nu)}$  and  $M^{(0N)}$  using the HFB wave functions in conjunction with  $PQQ1$ ,  $PQQHH1$ ,  $PQQ2$  and  $PQQHH2$  interaction and three different parameterizations of the Jastrow type of SRC for  $^{96}\text{Ru}$ ,  $^{102}\text{Pd}$ ,  $^{106}\text{Cd}$ ,  $^{124}\text{Xe}$ ,  $^{130}\text{Ba}$  and  $^{156}\text{Dy}$  nuclei are given in Table I. The sets of twelve NTMEs  $M^{(0\nu)}$  and  $M^{(0N)}$  are calculated in the approximation of finite size of nucleons with dipole form factor (F) and finite size plus SRC (F+S). Further, the NTMEs  $M^{(0\nu)}$  are calculated for  $\bar{A}$  and  $\bar{A}/2$  in the energy denominator in the case of F+S. We present the components of NTMEs  $M^{(0\nu)}$  as well as  $M^{(0N)}$ , namely Fermi, Gamow-Teller and tensor matrix elements of  $^{106}\text{Cd}$  in Table II for explicitly displaying the role of higher order currents (HOC). In Table III, the changes in NTMEs  $M^{(0\nu)}$  and  $M^{(0N)}$ , due to different approximations are displayed. The following observations are noteworthy.

- (i) Changing  $\bar{A}$  to  $\bar{A}/2$  in the energy denominator, the changes in the NTMEs  $M^{(0\nu)}$  vary between 9%–12 % exhibiting that the dependence of NTMEs on average excitation energy  $\bar{A}$  is small, which supports the use of the closure approximation in the case of the  $(\beta\beta)_{0\nu}$  decay.
- (ii) Inclusion of effects due to FNS induces changes in the NTMEs  $M_{VV}^{(0\nu)} + M_{AA}^{(0\nu)}$  by 9.0%–13.0%. Further, the addition of higher order currents (HOC) reduces the NTMEs by 11.0%–15.0%.
- (iii) With the addition of SRC1, SRC2 and SRC3, the NTMEs  $M^{(0\nu)}$  vary approximately by 13%–20%, 0.9%–2.6% and 2.5%–3.0%, respectively, in comparison to the case F.
- (iv) The NTMEs  $M_{VV}^{(0N)} + M_{AA}^{(0N)}$  in the case of heavy neutrino exchange, with the consideration of FNS instead of point nucleons, vary by 18.0%–29.0%, and the inclusion of HOC results in further reduction by about 14.0%–17.5%.
- (v) In the case of heavy neutrino exchange, the NTMEs  $M^{(0N)}$  become smaller by approximately 65%–

TABLE I: Calculated NTMEs  $M^{(0\nu)}$  and  $M^{(0N)}$  in the PHFB model with four different parameterization of effective two-body interaction, namely (a)  $PQQ1$ , (b)  $PQQHH1$ , (c)  $PQQ2$  and (d)  $PQQHH2$  and three different parameterizations of Jastrow type of SRC for the  $(\beta^+\beta^+)_{0\nu}$  and  $(\varepsilon\beta^+)_{0\nu}$  modes of  $^{96}\text{Ru}$ ,  $^{102}\text{Pd}$ ,  $^{106}\text{Cd}$ ,  $^{124}\text{Xe}$ ,  $^{130}\text{Ba}$  and  $^{156}\text{Dy}$  isotopes due to the exchange of light as well as heavy Majorana neutrinos. See footnote on p.3 of Ref. [35] for further details.

Nuclei		Light neutrino exchange							Heavy neutrino exchange			
		F	F+S			F+S(A/2)			F	F+S		
			SRC1	SRC2	SRC3	SRC1	SRC2	SRC3		SRC1	SRC2	SRC3
$^{96}\text{Ru}$	(a)	4.7979	4.1538	4.7331	4.9191	4.5739	5.1844	5.3777	251.3551	87.5090	150.6483	205.2102
	(b)	4.7820	4.1352	4.7164	4.9032	4.5501	5.1626	5.3567	252.6125	88.1241	151.5084	206.2858
	(c)	4.8334	4.1861	4.7686	4.9555	4.6107	5.2245	5.4187	252.8381	88.1649	151.6459	206.4813
	(d)	4.7399	4.1000	4.6753	4.8601	4.5120	5.1182	5.3103	250.2061	87.4415	150.1862	204.3879
$^{102}\text{Pd}$	(a)	5.3695	4.5877	5.2981	5.5230	5.0512	5.8007	6.0346	296.4236	97.6551	174.1164	240.2760
	(b)	4.5052	3.8203	4.4407	4.6377	4.1853	4.8400	5.0449	261.2562	87.2707	154.2305	212.1479
	(c)	5.4006	4.6167	5.3292	5.5547	5.0831	5.8348	6.0694	297.6968	98.3279	175.0482	241.4044
	(d)	4.4595	3.7823	4.3959	4.5907	4.1432	4.7907	4.9933	258.6259	86.5570	152.7985	210.0766
$^{106}\text{Cd}$	(a)	8.4560	7.2607	8.3403	8.6835	8.0547	9.1947	9.5519	452.6855	149.5474	265.9923	366.9093
	(b)	6.9410	5.9037	6.8370	7.1347	6.5165	7.5021	7.8119	394.7635	132.0821	233.0127	320.4765
	(c)	8.5399	7.3370	8.4229	8.7683	8.1436	9.2902	9.6497	455.6637	150.6151	267.7800	369.3362
	(d)	7.7425	6.6175	7.6293	7.9524	7.3228	8.3911	8.7274	428.1103	143.0153	252.5179	347.4477
$^{124}\text{Xe}$	(a)	4.1442	3.5405	4.0770	4.2507	3.9471	4.5153	4.6966	230.5375	76.6774	135.6415	186.8959
	(b)	3.4015	2.8367	3.3342	3.4963	3.1370	3.6639	3.8331	213.1788	70.0146	124.7059	172.4178
	(c)	3.6899	3.1428	3.6275	3.7849	3.5024	4.0157	4.1799	207.7699	68.5459	121.8099	168.1977
	(d)	3.4722	2.8994	3.4045	3.5690	3.2056	3.7406	3.9123	216.5439	71.2281	126.7645	175.1900
$^{130}\text{Ba}$	(a)	3.5986	3.0605	3.5369	3.6914	3.4204	3.9254	4.0868	205.5885	68.6378	121.1524	166.7736
	(b)	2.8901	2.4039	2.8372	2.9769	2.6473	3.1067	3.2525	186.0534	62.0004	109.6716	150.9816
	(c)	2.9496	2.4910	2.8950	3.0266	2.7799	3.2083	3.3457	174.2028	57.7641	102.3282	141.1255
	(d)	1.5194	1.2183	1.4801	1.5662	1.3358	1.6133	1.7032	110.7898	34.9642	63.7693	89.0510
$^{156}\text{Dy}$	(a)	2.1901	1.9136	2.1712	2.2513	2.1304	2.4044	2.4882	112.6022	39.8413	68.3273	92.5002
	(b)	1.9284	1.6658	1.9097	1.9857	1.8415	2.1010	2.1805	106.1906	37.2359	64.1897	87.1017
	(c)	2.5208	2.1991	2.4982	2.5913	2.4520	2.7702	2.8675	130.9372	46.4436	79.5200	107.5918
	(d)	2.5789	2.2241	2.5526	2.6551	2.4674	2.8168	2.9241	142.7229	49.7900	86.0621	116.9468

TABLE II: Decomposition of NTMEs  $M^{(0\nu)}$  and  $M^{(0N)}$  for the  $(\beta^+\beta^+)_{0\nu}$  and  $(\varepsilon\beta^+)_{0\nu}$  modes of  $^{106}\text{Cd}$  including finite size effect (F) and SRC (F+S) for the  $PQQ1$  parameterization.

NTMEs	Light neutrino exchange ( $K = 0\nu$ )				Heavy neutrino exchange ( $K = 0N$ )			
	F	F+S			F	F+S		
		SRC1	SRC2	SRC3		SRC1	SRC2	SRC3
$M_F^{(K)}$	2.6164	2.2956	2.6164	2.7064	133.9749	69.7853	105.3773	125.4157
$M_{GT-AA}^{(K)}$	-7.8995	-6.7491	-7.7996	-8.1279	-461.3370	-179.9510	-301.7550	-393.8500
$M_{GT-AP}^{(K)}$	-.5562	-.3643	-.5003	-.5570	218.6080	55.4365	118.4700	172.6570
$M_{GT-PP}^{(K)}$	1.8965	1.3980	1.7872	1.9323	-83.4189	-11.3250	-36.4994	-60.7425
$M_{GT-MM}^{(K)}$	-.2945	-.1479	-.2276	-.2735	-52.2544	20.1072	9.1939	-16.8909
$M_{GT}^{(K)}$	-6.8537	-5.8634	-6.7404	-7.0261	-378.4023	-115.7323	-210.5905	-298.8264
$M_{T-AP}^{(K)}$	-.0306	-.0311	-.0319	-.0318	14.8474	14.5508	15.8270	15.8681
$M_{T-PP}^{(K)}$	.0835	.0849	.0866	.0864	-5.9893	-5.8221	-6.4169	-6.4410
$M_{T-MM}^{(K)}$	.0087	.0087	.0092	.0091	2.0565	1.8336	2.2001	2.2449
$M_T^{(K)}$	.0615	.0625	.0638	.0637	10.9146	10.5624	11.6101	11.6720
$ M^{(K)} $	8.4560	7.2607	8.3403	8.6835	452.6855	149.5474	265.9923	366.9093

TABLE III: Changes (in %) of the NTMEs  $M^{(0\nu)}$  and  $M^{(0N)}$  due to exchange of light and heavy Majorana neutrinos, respectively, for the  $(\beta^+\beta^+)_{0\nu}$  and  $(\varepsilon\beta^+)_{0\nu}$  modes with the inclusion of finite size effect (FNS) as well as finite size effect+HOC (F), F+SRC (F+SRC1, F+SRC2 and F+SRC3) for four different parameterizations of the effective two-body interaction.

	Light neutrino exchange			Heavy neutrino exchange		
	FNS	F	F+S	FNS	F	F+S
(a)	9.08–10.31	10.91–12.47	12.63–14.95 0.86–1.72 2.53–2.86	25.89–28.91	14.41–17.51	64.62–67.06 39.32–41.26 17.85–18.95
(b)	9.58–11.34	10.87–13.39	13.53–16.82 0.97–1.98 2.53–3.00	26.03–29.23	14.25–16.75	64.93–67.16 39.55–41.50 17.98–19.12
(c)	9.18–10.63	10.88–12.43	12.76–15.55 0.89–1.85 2.53–2.85	25.96–29.17	14.35–17.40	64.53–67.01 39.27–41.37 17.83–19.05
(d)	9.57–12.74	10.84–14.91	13.50–19.81 1.02–2.59 2.54–3.08	26.18–29.80	14.19–17.46	65.05–68.44 39.70–42.44 18.06–19.62

68%, 39%–42% and 18%–20% for SRC1, SRC2 and SRC3, respectively. To understand the behaviour of SRC, we plot in Fig. 1 the neutrino potential  $H_N(r, \Lambda) = H_F^{(0N)}(r, \Lambda) f^2(r)$  with three different parameterizations of the SRC. The potential including only FNS is peaked at origin whereas the peaks due to F+SRC1, F+SRC2 and F+SRC3 are at  $r \approx 0.8$  fm, 0.7 fm and 0.5 fm, respectively. The visible reduction of the area under the curves is the main cause behind the large changes reported in Table III.

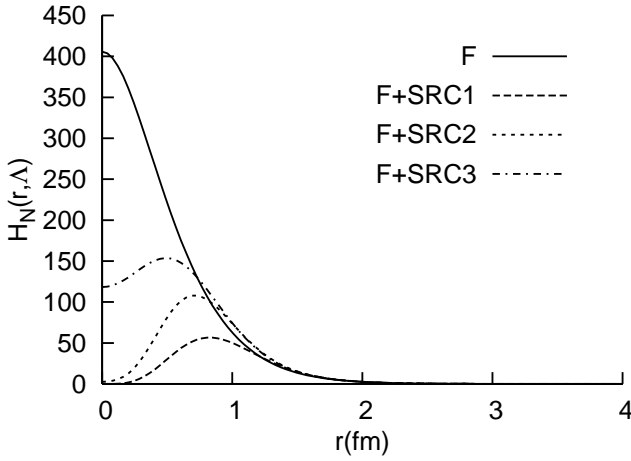


FIG. 1: Radial dependence of  $H_N(r, \Lambda) = H_F^{(0N)}(r, \Lambda) f^2(r)$  for the three different parameterizations of the SRC. In the case of FNS,  $f(r) = 1$ .

- (vi) The maximum variations in  $M^{(0\nu)}$  ( $M^{(0N)}$ ) due to  $PQQHH1$ ,  $PQQ2$  and  $PQQHH2$  parameterizations with respect to  $PQQ1$  interaction, but for the pathological case  $^{130}\text{Ba}$ , are about 21.0% (13.0%), 19.0% (17.0%) and 18.0% (27.0%).
- (vii) The effect of deformation on  $M^{(K)}$  is quantified by

the quantity  $D^{(K)}$  as the ratio of  $M^{(K)}$  at zero deformation ( $\zeta_{qq} = 0$ ) and full deformation ( $\zeta_{qq} = 1$ ) and is given by [34]

$$D^{(K)} = \frac{M^{(K)}(\zeta_{qq} = 0)}{M^{(K)}(\zeta_{qq} = 1)} \quad (16)$$

In Table IV, we tabulate the values of  $D^{(K)}$  due to exchange of light and heavy neutrinos for  $^{96}\text{Ru}$ ,  $^{102}\text{Pd}$ ,  $^{106}\text{Cd}$ ,  $^{124}\text{Xe}$ ,  $^{130}\text{Ba}$  and  $^{156}\text{Dy}$  nuclei. It is observed that, due to deformation effects, the NTMEs  $M^{(K)}$  are suppressed by factor of 1.7–10.8 in the mass range  $A = 96 - 156$ . Thus, the deformation plays a crucial role in the  $(\beta^+\beta^+)_{0\nu}$  and  $(\varepsilon\beta^+)_{0\nu}$  modes.

- (viii) It is also observed that excluding the pathological case  $^{130}\text{Ba}$  the ratios of NTMEs  $M^{(0\nu)}/M^{(0N)}$  are about 21–25, 32–37 and 42–49 for SRC1, SRC2 and SRC3, respectively. The spread in the above mentioned ratios increases to 21–29, 32–43 and 42–57 with the consideration of  $^{130}\text{Ba}$  isotope.

## B. Radial evolution of NTMEs

In the Majorana neutrino mass mechanism, the radial evolution of NTMEs can be studied by defining

$$M^{(K)} = \int C^{(K)}(r) dr. \quad (17)$$

The study of radial evolution of NTMEs  $M^{(0\nu)}$  in the QRPA by Šimkovic *et al.* [42], and in the ISM by Menéndez *et al.* [58], has established that the magnitude of  $C^{(0\nu)}$  for all nuclei undergoing  $(\beta^-\beta^-)_{0\nu}$  decay exhibit a maximum at about the internucleon distance  $r \approx 1$  fm, and that the contributions of decaying pairs coupled to  $J = 0$  and  $J > 0$  almost cancel out beyond

TABLE IV: Deformation ratios  $(i) D^{(0\nu)}$  and  $(ii) D^{(0N)}$  of  $(\beta^+\beta^+)_{0\nu}$  and  $(\varepsilon\beta^+)_{0\nu}$  modes for the  $PQQ1$  parameterization.

Nuclei		F	F+SRC		
			F+SRC1	F+SRC2	F+SRC3
$^{96}\text{Ru}$	(i)	2.53	2.54	2.53	2.53
	(ii)	2.44	2.34	2.40	2.43
$^{102}\text{Pd}$	(i)	2.68	2.74	2.68	2.67
	(ii)	2.40	2.45	2.42	2.40
$^{106}\text{Cd}$	(i)	1.92	1.96	1.93	1.92
	(ii)	1.72	1.77	1.74	1.73
$^{124}\text{Xe}$	(i)	3.82	3.92	3.84	3.82
	(ii)	3.36	3.50	3.42	3.38
$^{130}\text{Ba}$	(i)	4.61	4.75	4.65	4.61
	(ii)	3.97	4.15	4.06	4.01
$^{156}\text{Dy}$	(i)	10.78	10.82	10.76	10.75
	(ii)	10.25	10.01	10.14	10.20

$r \approx 3$  fm. In the PHFB model, the radial evolution of NTMEs  $M^{(0\nu)}$  and  $M^{(0N)}$  for  $(\beta^-\beta^-)_{0\nu}$  decay due to the exchange of light [35] and heavy Majorana neutrinos [36] has also been studied and similar observations have been reported.

Presently, we study the radial dependence of  $C^{(0\nu)}$  as well as  $C^{(0N)}$  for  $(\beta^+\beta^+)_{0\nu}$  and  $(\varepsilon\beta^+)_{0\nu}$  modes of  $^{96}\text{Ru}$ ,  $^{102}\text{Pd}$ ,  $^{106}\text{Cd}$ ,  $^{124}\text{Xe}$ ,  $^{130}\text{Ba}$  and  $^{156}\text{Dy}$  isotopes in four cases, namely F, F+SRC1, F+SRC2 and F+SRC3. In Fig. 2 we plot the radial dependence of  $C^{(0\nu)}$  and  $C^{(0N)}$  for  $^{106}\text{Cd}$ , employing the  $PQQ1$  parameterization of the effective two body interaction, for four combinations of FNS and SRC. In Fig. 3, the radial evolution of  $C^{(0\nu)}$  and  $C^{(0N)}$  are displayed together for the six nuclei under study, for the four combinations of FNS and SRC.

In the case of light Majorana neutrino exchange, it is noticed that the  $C^{(0\nu)}$  are peaked at  $r = 1.0$  fm for finite size nucleons and the addition of SRC1 and SRC2 shifts the peak to 1.25 fm. However, the position of the peak remains unchanged at  $r = 1.0$  fm with the inclusion of SRC3. The radial distributions of  $C^{(0\nu)}$  extends up to 10 fm although the maximum contribution to  $M^{(0\nu)}$  results from the distribution up to 3 fm. In the case of heavy Majorana neutrino exchange, the  $C^{(0N)}$  are peaked at  $r \approx 0.5$  fm in the case of FNS, and with the addition of SRC1 and SRC2, the peak shifts to about 0.8 fm, and to 0.7 fm for SRC3. The radial distributions of  $C^{(0N)}$  extend up to 2 fm and the total distribution contributes to the evolution of  $M^{(0N)}$ . Remarkably, the above observations also remain valid with the other three parameterizations of the effective two-body interaction.

### C. Uncertainties in nuclear transition matrix elements and nuclear sensitivity

The uncertainties associated with the NTMEs  $M^{(0\nu)}$  and  $M^{(0N)}$  for  $(\beta^+\beta^+)_{0\nu}$  and  $(\varepsilon\beta^+)_{0\nu}$  modes of  $^{96}\text{Ru}$ ,  $^{102}\text{Pd}$ ,  $^{106}\text{Cd}$ ,  $^{124}\text{Xe}$ ,  $^{130}\text{Ba}$  and  $^{156}\text{Dy}$  isotopes due to

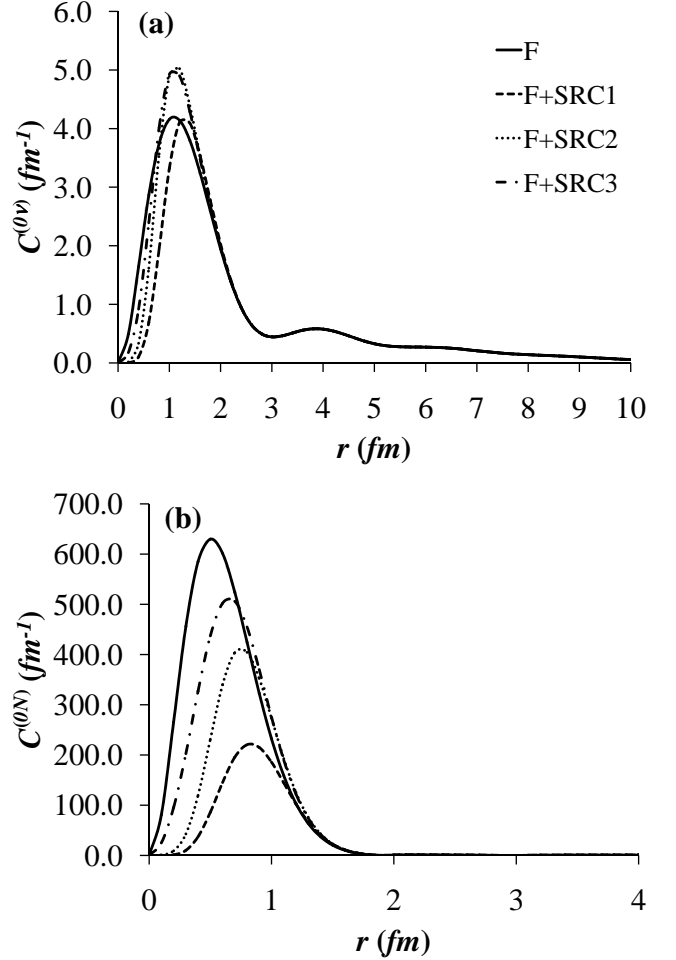


FIG. 2: Radial dependence of  $C^{(0\nu)}(r)$  and  $C^{(0N)}(r)$  for the  $(\beta^+\beta^+)_{0\nu}$  and  $(\varepsilon\beta^+)_{0\nu}$  modes of  $^{106}\text{Cd}$  isotope.

the exchange of light and heavy neutrinos, respectively are evaluated by calculating the mean and standard deviation given by

$$\overline{M}^{(K)} = \frac{\sum_{i=1}^N M_i^{(K)}}{N} \quad (18)$$

and

$$\Delta \overline{M}^{(K)} = \frac{1}{\sqrt{N-1}} \left[ \sum_{i=1}^N \left( \overline{M}^{(K)} - M_i^{(K)} \right)^2 \right]^{1/2}. \quad (19)$$

The twelve NTMEs due to the exchange of light as well as heavy Majorana neutrinos listed in the three columns 4–6 and 11–13 (F+S) of Table I are employed in this statistical analysis for the bare and quenched values of axial vector coupling constant  $g_A = 1.254$  and  $g_A = 1.0$ , respectively. Further, the effect due to the Miller-Spenser parameterization of Jastrow type of SRC is estimated by evaluating the same mean  $\overline{M}^{(K)}$  and their standard deviations  $\Delta \overline{M}^{(K)}$  for eight NTMEs calculated using SRC2

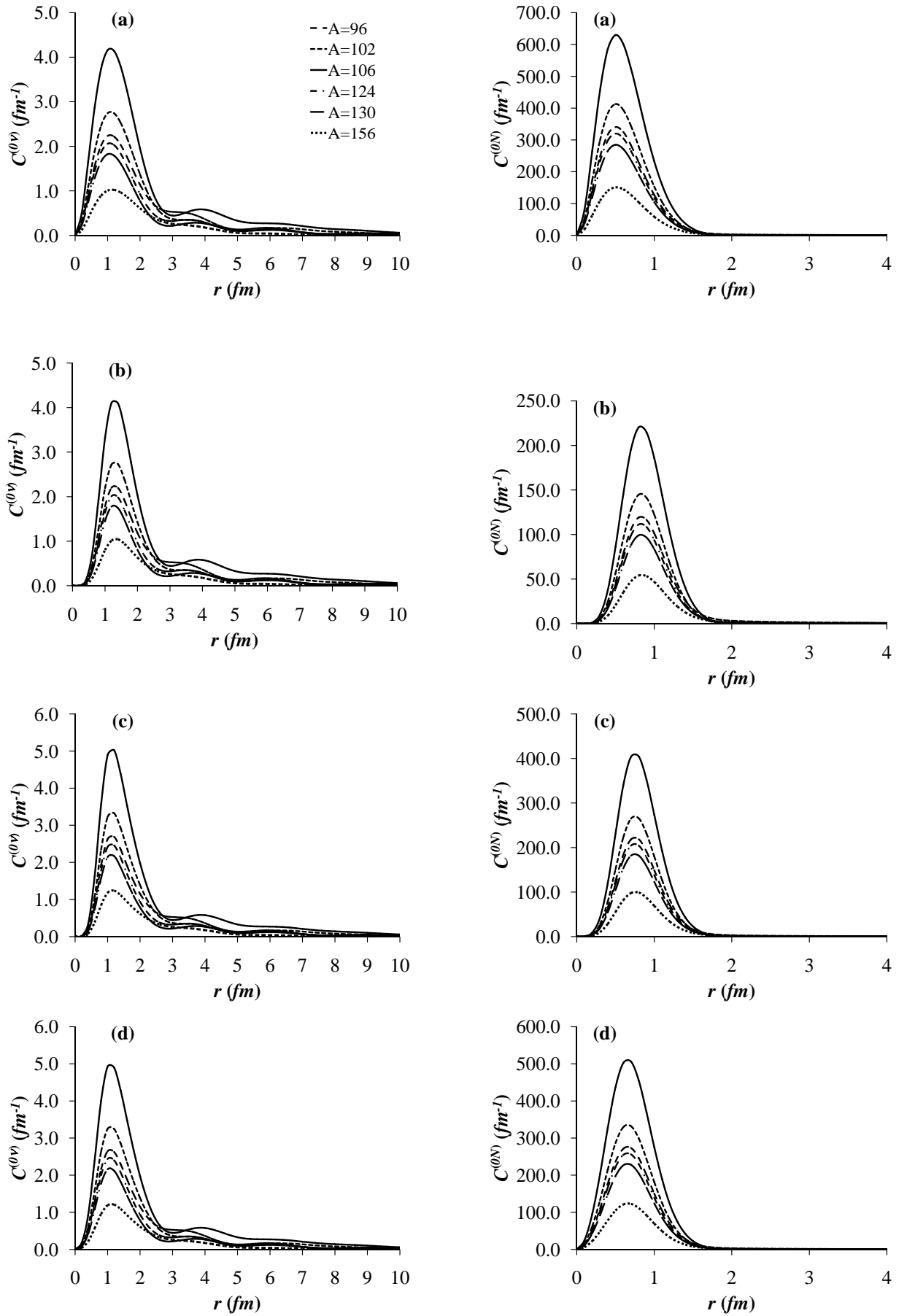


FIG. 3: Radial dependence of  $C^{(0\nu)}(r)$  (left) and  $C^{(0N)}(r)$  (right) for the  $(\beta^+\beta^+)_{0\nu}$  and  $(\varepsilon\beta^+)_{0\nu}$  modes of  $^{96}\text{Ru}$ ,  $^{102}\text{Pd}$ ,  $^{106}\text{Cd}$ ,  $^{124}\text{Xe}$ ,  $^{130}\text{Ba}$  and  $^{156}\text{Dy}$  isotopes. In this Fig., (a), (b), (c) and (d) correspond to F, F+SRC1, F+SRC2 and F+SRC3, respectively.



TABLE V: Average NTMEs  $\overline{M}^{(K)}$  and uncertainties  $\Delta\overline{M}^{(K)}$  for  $(\beta^+\beta^+)_{0\nu}$  and  $(\varepsilon\beta^+)_{0\nu}$  modes of  $^{96}\text{Ru}$ ,  $^{102}\text{Pd}$ ,  $^{106}\text{Cd}$ ,  $^{124}\text{Xe}$ ,  $^{130}\text{Ba}$  and  $^{156}\text{Dy}$  isotopes. Both bare and quenched values of  $g_A$  are considered. Case I and Case II denote calculations with and without SRC1, respectively. In column 9, (l) and (s) denote large and small basis, respectively.

Nuclei	$g_A$	Light neutrino exchange								Heavy neutrino exchange			
		Case I		Case II		QRPA [23]	QRPA [59]	SQRPA [60]	MCM [61]	Case I		Case II	
		$\overline{M}^{(0\nu)}$	$\Delta\overline{M}^{(0\nu)}$	$\overline{M}^{(0\nu)}$	$\Delta\overline{M}^{(0\nu)}$					$\overline{M}^{(0N)}$	$\Delta\overline{M}^{(0N)}$	$\overline{M}^{(0N)}$	$\Delta\overline{M}^{(0N)}$
$^{96}\text{Ru}$	1.254	4.59	0.34	4.82	0.11	3.60	4.228		2.383	148.13	50.27	178.29	29.19
	1.0	5.13	0.40	5.39	0.13					165.91	59.74	201.49	35.61
$^{102}\text{Pd}$	1.254	4.71	0.60	4.97	0.50					160.83	58.13	195.01	35.86
	1.0	5.34	0.71	5.63	0.59					181.01	69.02	221.36	43.39
$^{106}\text{Cd}$	1.254	7.57	0.89	7.97	0.72	4.56	4.778	7.85(l)	3.394	249.89	89.73	302.93	54.54
	1.0	8.52	1.04	8.98	0.84			8.17(s)		281.22	106.57	343.82	66.13
$^{124}\text{Xe}$	1.254	3.50	0.42	3.69	0.32	5.27	2.975		8.301	124.84	44.75	151.45	26.71
	1.0	3.96	0.49	4.19	0.37					140.70	53.16	172.11	32.44
$^{130}\text{Ba}$	1.254	2.60	0.80	2.75	0.82	5.52	5.579		5.130	97.35	41.65	118.11	34.03
	1.0	2.94	0.90	3.12	0.92					109.75	48.71	134.24	39.56
$^{156}\text{Dy}$	1.254	2.22	0.31	2.33	0.29					72.96	26.36	87.78	18.02
	1.0	2.50	0.36	2.63	0.33					81.66	31.12	99.13	21.41

TABLE VI: Limits on the effective mass of light  $\langle m_\nu \rangle$  and heavy  $\langle M_N \rangle$  Majorana neutrinos for the  $(\beta^+\beta^+)_{0\nu}$  and  $(\varepsilon\beta^+)_{0\nu}$  modes of  $^{96}\text{Ru}$ ,  $^{102}\text{Pd}$ ,  $^{106}\text{Cd}$ ,  $^{124}\text{Xe}$ ,  $^{130}\text{Ba}$  and  $^{156}\text{Dy}$  isotopes.

$e^+\beta\beta$ emitters	$T_{1/2}^{0\nu}$ (yr)		Ref.	$g_A$	$\langle m_\nu \rangle$ (eV)		$\langle M_N \rangle$ (GeV)	
	$\beta^+\beta^+$	$\varepsilon\beta^+$			$\beta^+\beta^+$	$\varepsilon\beta^+$	$\beta^+\beta^+$	$\varepsilon\beta^+$
$^{96}\text{Ru}$	$>3.1\times 10^{16}$	$>6.7\times 10^{16}$	[62]	1.254 1.0	$4.02\times 10^5$ $5.66\times 10^5$	$7.94\times 10^4$ $1.12\times 10^5$	$4.41\times 10$ $3.17\times 10$	$2.23\times 10^2$ $1.61\times 10^2$
$^{106}\text{Cd}$	$>1.2\times 10^{21}$	$>2.2\times 10^{21}$	[14]	1.254 1.0	$1.16\times 10^3$ $1.62\times 10^3$	$2.27\times 10^2$ $3.16\times 10^2$	$1.57\times 10^4$ $1.13\times 10^4$	$8.04\times 10^4$ $5.80\times 10^4$
$^{124}\text{Xe}$	$>4.2\times 10^{17}$	$>1.2\times 10^{18}$	[63]	1.254 1.0	$1.22\times 10^5$ $1.70\times 10^5$	$1.68\times 10^4$ $2.33\times 10^4$	$1.61\times 10^2$ $1.16\times 10^2$	$1.17\times 10^3$ $8.46\times 10^2$
$^{130}\text{Ba}$	$>4.0\times 10^{21}$	$>4.0\times 10^{21}$	[64]	1.254 1.0	$4.11\times 10^3$ $5.70\times 10^3$	$4.19\times 10^2$ $5.82\times 10^2$	$5.01\times 10^3$ $3.62\times 10^3$	$4.91\times 10^4$ $3.55\times 10^4$

and SRC3 parameterizations. In Table V, we display the calculated averages and their variances along with all the available theoretical results in other models for  $^{96}\text{Ru}$ ,  $^{102}\text{Pd}$ ,  $^{106}\text{Cd}$ ,  $^{124}\text{Xe}$ ,  $^{130}\text{Ba}$  and  $^{156}\text{Dy}$  isotopes.

In the case of light Majorana neutrino exchange, it is observed that the uncertainties  $\Delta\overline{M}^{(0\nu)}$  but for  $^{130}\text{Ba}$  are about 7%–14% and the exclusion of NTMEs  $M^{(0\nu)}$  calculated with the Miller-Spencer parameterization of Jastrow SRC, reduces the uncertainties to 2%–12% for both  $g_A = 1.254$  and  $g_A = 1.0$ . Pathologically, the uncertainty  $\Delta\overline{M}^{(0\nu)} \approx 30\%$  in the case of  $^{130}\text{Ba}$ , remain unaltered due to the large effects of  $PQQHH2$  parameterization. The estimated uncertainties  $\Delta\overline{M}^{(0\nu)}$  but for  $^{130}\text{Ba}$  isotope in the heavy Majorana neutrino mass mechanism, are about 35% for  $g_A = 1.254$  and  $g_A = 1.0$ . Estimation

of uncertainties for eight NTMEs  $\overline{M}^{(0N)}$  calculated using the SRC2 and SRC3 parameterizations again reveal that the  $\Delta\overline{M}^{(0N)}$  are reduced to 16%–21% due to the exclusion of SRC1. In  $^{130}\text{Ba}$  isotope, the same pathological behaviour is noticed.

In the QRPA calculations of Hirsch *et al.* [23] and Staudt *et al.* [59], the NTMEs  $M^{(0\nu)}$  are almost identical but for  $^{124}\text{Xe}$ , in which the difference is approximately by a factor of 1.8. Stoica *et al.* [60] have used SQRPA model with two model spaces, namely small basis (oscillator shells of  $3\hbar\omega - 5\hbar\omega + i_{13/2}$  orbit) and a large basis (oscillator shells of  $2\hbar\omega - 5\hbar\omega + i_{13/2}$  orbit). They used the same SPEs as those of Hirsch *et al.* and an effective two-body interaction derived from the Bonn-A potential. The NTMEs calculated in the SQRPA [60] do not depend much on the model space and differ by a factor of 1.8 ap-

TABLE VII: Predicted half-lives, corresponding extracted effective mass of heavy Majorana neutrino  $\langle M_N \rangle$ , nuclear sensitivities  $\xi^{(0\nu)}$  and  $\xi^{(0N)}$  due to exchange of light and heavy neutrino, respectively, for  $(\beta^+\beta^+)_{0\nu}$  and  $(\varepsilon\beta^+)_{0\nu}$  modes of  $^{96}\text{Ru}$ ,  $^{102}\text{Pd}$ ,  $^{106}\text{Cd}$ ,  $^{124}\text{Xe}$ ,  $^{130}\text{Ba}$  and  $^{156}\text{Dy}$  isotopes.

$e^+\beta\beta$ emitters	$g_A$	$T_{1/2}^{0\nu} (\langle m_\nu \rangle = 0.05 \text{ eV})$		$\langle M_N \rangle \text{ (GeV)}$	$\xi^{(0\nu)}$		$\xi^{(0N)}$	
		$\beta^+\beta^+$	$\varepsilon\beta^+$		$\beta^+\beta^+$	$\varepsilon\beta^+$	$\beta^+\beta^+$	$\varepsilon\beta^+$
$^{96}\text{Ru}$	1.254	$2.01^{+0.09}_{-0.09} \times 10^{30}$	$1.69^{+0.08}_{-0.07} \times 10^{29}$	$3.55^{+0.58}_{-0.58} \times 10^8$	0.721	2.486	26.70	92.02
	1.0	$3.97^{+0.19}_{-0.18} \times 10^{30}$	$3.34^{+0.16}_{-0.15} \times 10^{29}$	$3.59^{+0.63}_{-0.63} \times 10^8$	0.513	1.768	19.19	66.13
$^{102}\text{Pd}$	1.254	-	$7.04^{+1.66}_{-1.23} \times 10^{30}$	$3.76^{+0.69}_{-0.69} \times 10^{8\dagger}$	-	0.385	-	15.11
	1.0	-	$1.36^{+0.34}_{-0.25} \times 10^{31}$	$3.77^{+0.74}_{-0.74} \times 10^{8\dagger}$		0.277		10.90
$^{106}\text{Cd}$	1.254	$6.49^{+1.34}_{-1.03} \times 10^{29}$	$4.52^{+0.94}_{-0.71} \times 10^{28}$	$3.64^{+0.66}_{-0.66} \times 10^8$	1.268	4.806	48.20	182.6
	1.0	$1.27^{+0.28}_{-0.21} \times 10^{30}$	$8.81^{+1.92}_{-1.45} \times 10^{28}$	$3.67^{+0.71}_{-0.71} \times 10^8$	0.908	3.442	34.79	131.8
$^{124}\text{Xe}$	1.254	$2.51^{+0.51}_{-0.39} \times 10^{30}$	$1.35^{+0.27}_{-0.21} \times 10^{29}$	$3.93^{+0.69}_{-0.69} \times 10^8$	0.645	2.777	26.44	113.9
	1.0	$4.84^{+1.00}_{-0.76} \times 10^{30}$	$2.61^{+0.54}_{-0.41} \times 10^{29}$	$3.94^{+0.74}_{-0.74} \times 10^8$	0.465	2.001	19.11	82.30
$^{130}\text{Ba}$	1.254	$2.70^{+2.76}_{-1.09} \times 10^{31}$	$2.82^{+2.88}_{-1.14} \times 10^{29}$	$4.12^{+1.19}_{-1.19} \times 10^8$	0.197	1.926	8.45	82.68
	1.0	$5.20^{+5.31}_{-2.11} \times 10^{31}$	$5.42^{+5.54}_{-2.20} \times 10^{29}$	$4.13^{+1.22}_{-1.22} \times 10^8$	0.142	1.387	6.11	59.76
$^{156}\text{Dy}$	1.254	-	$5.94^{+1.79}_{-1.23} \times 10^{29}$	$3.62^{+0.74}_{-0.74} \times 10^{8\dagger}$	-	1.327	-	50.04
	1.0	-	$1.15^{+0.35}_{-0.24} \times 10^{30}$	$3.61^{+0.78}_{-0.78} \times 10^{8\dagger}$		0.953		35.94

$^{\dagger}$  denotes  $(\varepsilon\beta^+)_{0\nu}$  mode only.

proximately from those of Hirsch *et al.* [23].

There are no available theoretical results and experimental half-life limits for the  $^{102}\text{Pd}$  and  $^{156}\text{Dy}$  isotopes. The extracted limits on the effective light neutrino mass  $\langle m_\nu \rangle$  as well as heavy neutrino mass  $\langle M_N \rangle$  using the phase space factors given in Ref. [34] and presently available experimental limits on observed half-lives of  $(\beta^+\beta^+)_{0\nu}$  and  $(\varepsilon\beta^+)_{0\nu}$  modes are presented in Table VI. The extracted limits on  $\langle m_\nu \rangle$  and  $\langle M_N \rangle$  are not so much stringent as in the case of  $(\beta^-\beta^-)_{0\nu}$  decay. Moreover, better limits are obtained in the case of  $(\varepsilon\beta^+)_{0\nu}$  mode even for equal limits on half-lives of  $(\beta^+\beta^+)_{0\nu}$  and  $(\varepsilon\beta^+)_{0\nu}$  modes. The best obtained limits for  $^{106}\text{Cd}$  isotope are  $\langle m_\nu \rangle < 1.16 \times 10^3$  ( $2.27 \times 10^2$ ) eV and  $\langle M_N \rangle < 1.57 \times 10^4$  ( $8.04 \times 10^4$ ) GeV in case of  $(\beta^+\beta^+)_{0\nu}$  and  $(\varepsilon\beta^+)_{0\nu}$  modes, respectively. In the case of  $(\beta^+\beta^+)_{0\nu}$  and  $(\varepsilon\beta^+)_{0\nu}$  modes, the extracted limits on the effective neutrino masses  $\langle m_\nu \rangle$  and  $\langle M_N \rangle$  are not stringent enough and hence, we calculate half-lives of these modes to be useful in the design of future experimental setups. The half-lives of  $(\beta^+\beta^+)_{0\nu}$  and  $(\varepsilon\beta^+)_{0\nu}$  modes for  $\langle m_\nu \rangle = 50 \text{ meV}$  are calculated and extracted corresponding limits on heavy neutrino mass,  $\langle M_N \rangle$ , are given in the same Table VII.

In the absence of stringent limits on the effective neutrino masses  $\langle m_\nu \rangle$  and  $\langle M_N \rangle$ , it is useful to calculate the nuclear sensitivity, defined as [40]

$$\xi^{(K)} = 10^8 \sqrt{G_{01}} |M^{(K)}| \quad (20)$$

where  $K$  stands for  $0\nu$  or  $0N$  mode and an arbitrary normalization factor  $10^8$  is introduced so that the nuclear sensitivity turns out to be order of unity.

It is observed that in general, nuclear sensitivities for  $(\varepsilon\beta^+)_{0\nu}$  mode are larger than those of  $(\beta^+\beta^+)_{0\nu}$  mode. Further, the nuclear sensitivities for  $(\beta^+\beta^+)_{0\nu}$  and  $(\varepsilon\beta^+)_{0\nu}$  modes of  $^{106}\text{Cd}$ ,  $^{96}\text{Ru}$  ( $^{124}\text{Xe}$ ),  $^{124}\text{Xe}$  ( $^{96}\text{Ru}$ ),  $^{130}\text{Ba}$ ,  $^{156}\text{Dy}$  and  $^{102}\text{Pd}$  isotopes, respectively, are in the decreasing order of their magnitudes.

#### IV. CONCLUSIONS

We have calculated sets of twelve NTMEs  $M^{(0\nu)}$  and  $M^{(0N)}$  for  $(\beta^+\beta^+)_{0\nu}$  and  $(\varepsilon\beta^+)_{0\nu}$  modes of  $^{96}\text{Ru}$ ,  $^{102}\text{Pd}$ ,  $^{106}\text{Cd}$ ,  $^{124}\text{Xe}$ ,  $^{130}\text{Ba}$  and  $^{156}\text{Dy}$  isotopes by employing the PHFB model with four different parameterizations of the pairing plus multipolar type of effective two body interaction and three different parameterizations of the short range correlations. To estimate statistically the uncertainties in NTMEs, mean and standard deviations of sets of twelve NTMEs  $M^{(0\nu)}$  and  $M^{(0N)}$  calculated with dipole form factor and short range correlations are employed for both  $g_A = 1.254$  and  $g_A = 1.0$ . It is observed that the largest standard deviation turns out to be around 30% in the case of  $^{130}\text{Ba}$  isotope due to the dominant contribution of deformation in  $PQQHH2$  parameterization. But for  $^{130}\text{Ba}$ , the maximum uncertainty in NTMEs  $M^{(0\nu)}$  is around 14%, which becomes smaller by 2% excluding the NTMEs calculated with SRC1 in the case of  $^{156}\text{Dy}$  isotope. The uncertainties in  $M^{(0N)}$  due to the exchange of heavy Majorana neutrino is about 35%. Exclusion of NTMEs calculated with SRC1, reduced the uncertainties by 14%–19%.

## Acknowledgments

This work is partially supported by the Council of Scientific and Industrial Research (CSIR), India vide sanction No. 03(1216)/12/EMR-II, Indo-Italian Collab-

oration DST-MAE project via grant no. INT/Italy/P-7/2012 (ER), Consejo Nacional de Ciencia y Tecnología (Conacyt)-México, and Dirección General de Asuntos del Personal Académico, Universidad Nacional Autónoma de México (DGAPA-UNAM) project IN103212.

- 
- [1] M. Doi and T. Kotani, Prog. Theor. Phys., **89** 139, (1993)
- [2] R. G. Winter, Phys. Rev. **100**, 142 (1955).
- [3] R. A. Eramzhyan, G. V. Micelmacher, and M. B. Voloshin, Pisma v ZhETF **35**, 530 (1982).
- [4] J. D. Vergados, Nucl. Phys. B **218**, 109 (1983).
- [5] J. Bernabeu, A. De Rujula, and C. Jarlskog, Nucl. Phys. B **223**, 15 (1983).
- [6] Z. Sujkowski and S. Wycech, Phys. Rev. C **70**, 052501(R) (2004).
- [7] L. Lukaszuk, Z. Sujkowski, and S. Wycech, Eur. Phys. J. A **27**, 63 (2006).
- [8] M. I. Krivoruchenko, F. Šimkovic, D. Frekers, and A. Faessler, Nucl. Phys. A **859**, 140 (2011).
- [9] J. D. Vergados, arXiv:1107.3296V2[hep-ph].
- [10] A. S. Barabash, Ph. Hubert, A. Nachab, and V. Umatov, Nucl. Phys. A **785**, 371 (2007).
- [11] D. Frekers, P. Puppe, J. H. Thies, P. P. Povinec, F. Šimkovic, J. Staniček, and I. Šýkora, Nucl. Phys. A **860**, 1 (2011).
- [12] P. Belli *et al.*, Eur. Phys. J. A **42**, 171 (2009).
- [13] N. I. Rukhadze *et al.*, Nucl. Phys. A **852**, 197 (2011); J. Phys.: Conf. Ser. 203, 012072 (2010).
- [14] P. Belli *et al.*, Phys. Rev. C **85**, 044610 (2012).
- [15] A. S. Barabash, Ph. Hubert, A. Nachab, S. I. Konovalov, I. A. Vanyushin, and V. Umatov, Nucl. Phys. A **807**, 269 (2008).
- [16] J. Dawson, R. Ramaswamy, C. Reeve, J. R. Wilson and, K. Zuber, Nucl. Phys. A **799**, 167 (2008).
- [17] J. Dawson, D. Degering, M. Köhler, R. Ramaswamy, C. Reeve, J. R. Wilson, and K. Zuber, Phys. Rev. C **78**, 035503 (2008).
- [18] M. F. Kidd, J. H. Esterline, and W. Tornow, Phys. Rev. C **78**, 035504 (2008).
- [19] A. S. Barabash, Ph. Hubert, A. Nachab, S. I. Konovalov, and V. Umatov, Phys. Rev. C **80**, 035501 (2009).
- [20] P. Belli, R. Bernabei, S. d'Angelo, F. Cappella, R. Cerulli, A. Incicchitti, M. Laubenstein, D. Prosperi, and V.I. Tretyak, Nuclear Physics A **824**, 101 (2009).
- [21] P. Belli, R. Bernabei, F. Cappella, R. Cerulli, F. A. Danevich, S. d'Angelo, A. Incicchitti, V. V. Kobychiev, D. V. Poda, V. I. Tretyak, J. Phys. G **38**, 115107 (2011).
- [22] H. V. Klapdor-Kleingrothaus, I. V. Krivosheina, and I. V. Titkova, Int. J. Mod. Phys. A **21**, 1159 (2006).
- [23] M. Hirsch, K. Muto, T. Oda, and H. V. Klapdor-Kleingrothaus, Z. Phys. A **347**, 151 (1994).
- [24] F. T. Avignone III, S. R. Elliott, and J. Engel, Rev. Mod. Phys. **80**, 481 (2008).
- [25] J. D. Vergados, H. Ejiri, and F. Šimkovic, arXiv:1205.0649v2[hep-ph].
- [26] A. Faessler, V. Rodin, F. Šimkovic, arXiv:1206.0464v1[nucl-th].
- [27] E. Caurier, A. Poves, and A. P. Zuker, Phys. Lett. **B252**, 13 (1990); E. Caurier, F. Nowacki, A. Poves, and J. Retamosa, Phys. Rev. Lett. **77**, 1954 (1996); Nucl. Phys. **A654**, 973c (1999); E. Caurier, F. Nowacki, and A. Poves, Eur. Phys. J. A **36**, 195 (2008).
- [28] E. Caurier, J. Menéndez, F. Nowacki, and A. Poves, Phys. Rev. Lett. **100**, 052503 (2008).
- [29] M. Horoi and S. Stoica, Phys. Rev. C **81**, 024321 (2010).
- [30] J. Suhonen and O. Civitarese, Phys. Rep. **300** 123 (1998).
- [31] A. Faessler, and F. Šimkovic, J. Phys. G **24**, 2139 (1998).
- [32] F. Šimkovic, L. Pacearescu, and A. Faessler, Nucl. Phys. A **733**, 321 (2004); L. Pacearescu, A. Faessler, and F. Šimkovic, Phys. At. Nucl. **67**, 1210 (2004); R. Álvarez-Rodríguez, P. Sarriguren, E. Moya de Guerra, L. Pacearescu, A. Faessler, and F. Šimkovic, Phys. Rev. C **70**, 064309 (2004); M. S. Yousef, V. Rodin, A. Faessler, and F. Šimkovic, Phys. Rev. C **79**, 014314 (2009).
- [33] D. Fang, A. Faessler, V. Rodin and F. Šimkovic, Phys. Rev. C **83**, 034320 (2011); Phys. Rev. C **82**, 051301(R) (2010).
- [34] P. K. Rath, R. Chandra, K. Chaturvedi, P. K. Raina, and J. G. Hirsch, Phys. Rev. C **80**, 044303 (2009).
- [35] P. K. Rath, R. Chandra, K. Chaturvedi, P. K. Raina, and J. G. Hirsch, Phys. Rev. C **82**, 064310 (2010).
- [36] P. K. Rath, R. Chandra, P. K. Raina, K. Chaturvedi, and J. G. Hirsch, Phys. Rev. C **85**, 014308 (2012).
- [37] J. G. Hirsch, O. Castaños, and P. O. Hess, Nucl. Phys. A **582**, 124 (1995).
- [38] J. Barea and F. Iachello, Phys. Rev. C **79**, 044301 (2009).
- [39] T. R. Rodríguez and G. Martínez-Pinedo, Phys. Rev. Lett. **105**, 252503 (2010).
- [40] F. Šimkovic, G. Pantis, J. D. Vergados, and A. Faessler, Phys. Rev. C **60**, 055502 (1999).
- [41] J. D. Vergados, Phys. Rep. **361**, 1 (2002).
- [42] F. Šimkovic, A. Faessler, V. Rodin, P. Vogel, and J. Engel, Phys. Rev. C **77**, 045503 (2008).
- [43] P. Vogel, in *Current Aspects of Neutrino Physics*, edited by D. O. Caldwell (Springer, 2001) Chap. 8, p. 177; arXiv: nucl-th/0005020.
- [44] John N. Bahcall, Hitoshi Murayama, and C. Peña-Garay, Phys. Rev. D **70**, 033012 (2004).
- [45] F. T. Avignone III, G. S. King III, and Yu. G. Zdesenko, New Journal of Physics **7**, 6 (2005).
- [46] S. M. Bilenky and J. A. Grifols, Phys. Lett. B **550**, 154 (2002).
- [47] V. A. Rodin, A. Faessler, F. Šimkovic, and P. Vogel, Phys. Rev. C **68**, 044302 (2003).
- [48] J. Suhonen, Phys. Lett. B **607**, 87 (2005).
- [49] V. A. Rodin, A. Faessler, F. Šimkovic, and P. Vogel, Nucl. Phys. A **766**, 107 (2006); **793**, 213 (2007).
- [50] M. Kortelainen and J. Suhonen, Phys. Rev. C **76**, 024315 (2007); M. Kortelainen, O. Civitarese, J. Suhonen, and J. Toivanen, Phys. Lett. B **647**, 128 (2007).
- [51] F. Šimkovic, A. Faessler, H. Mütter, V. Rodin, and M. Stauf, Phys. Rev. C **79**, 055501 (2009).
- [52] H. F. Wu, H. Q. Song, T. T. S. Kuo, W. K. Cheng, and D. Strottman, Phys. Lett. **B162**, 227 (1985).

- [53] G. A. Miller and J. E. Spencer, *Ann. Phys. (NY)* **100**, 562 (1976).
- [54] R. Chandra, K. Chaturvedi, P. K. Rath, P. K. Raina, and J. G. Hirsch, *Europhys. Lett.* **86**, 32001 (2009).
- [55] P. K. Raina, A. Shukla, S. Singh, P. K. Rath, and J. G. Hirsch, *Eur. Phys. J. A* **28**, 27 (2006); A. Shukla, P. K. Raina, R. Chandra, P. K. Rath, and J. G. Hirsch, *Eur. Phys. J. A* **23**, 235 (2005).
- [56] S. Singh, R. Chandra, P. K. Rath, P. K. Raina, and J. G. Hirsch, *Eur. Phys. J. A* **33**, 375 (2007).
- [57] P. K. Rath, R. Chandra, S. Singh, P. K. Raina, and J. G. Hirsch, *J. Phys. G* **37**, 055108 (2010).
- [58] J. Menéndez, A. Poves, E. Caurier, and F. Nowacki, *Nucl. Phys. A* **818**, 139 (2009).
- [59] A. Staudt, K. Muto, and H. V. Klapdor-Kleingrothaus, *Phys. Lett. B* **268**, 312 (1991).
- [60] S. Stoica and H. V. Klapdor-Kleingrothaus, *Eur. Phys. J. A* **17**, 529 (2003).
- [61] J. Suhonen and M. Aunola, *Nucl. Phys. A* **723**, 271 (2003).
- [62] Eric B. Norman, *Phys. Rev. C* **31**, 1937 (1985).
- [63] A. S. Barabash, V. V. Kuzminov, V. M. Lobashev, V. M. Novikov, B. M. Ovchinnikov, and A. A. Pomansky, *Phys. Lett. B* **223**, 273 (1989).
- [64] A. S. Barabash and R. R. Saakyan, *Phys. At. Nucl.* **59**, 179 (1996).